3B2v7.51c GML4.3.1 | OLEN : 2580 | Prod.Type:com pp.1–8(col.fig.:NIL) | ED:binny/brr PAGN: mva SCAN: mangala

ARTICLE IN PRESS

ELSEVIER

Optics and Lasers in Engineering 0 (▮▮▮▮) ▮▮▮–▮▮▮

OPTICS and LASERS in ENGINEERING

Separation of vibration fringe data from rotating object fringes using pulsed ESPI

Carlos Pérez López[a], Fernando Mendoza Santoyo[a,*], Ramón Rodríguez Vera[a], Marcelo Funes-Gallanzi[b]

[a] *Centro de Investigaciones en Optica, A.C., Loma del Bosque 115, León, Gto. 37150, Mexico*
[b] *Instituto Nacional de Astrofisica Optica y Electrónica, Luis Enrique Erro 1, Tonantzintla, Puebla, Pue. 72840, Mexico*

Abstract

In industrial and other types of non-controlled environments, an unbalanced rotating object may present characteristic out-of-plane vibration amplitude at a specific frequency. For this type of cases and as a first step towards a complete evaluation, it is only desired to visualize the effect of the vibration on the rotating object, or vice versa, for instance to achieve object balancing. Real time optical non-intrusive measurement techniques such as pulsed electronic speckle pattern interferometry (ESPI), are well suited to study this rotating-vibrating object. The advantage offered by ESPI is that real-time fringe data is qualitatively analyzed while being observed on a TV monitor. The present paper proposes a qualitative method, based on pulsed ESPI, to separate rotation fringes from fringes solely related to vibration. The method relies on a high precision scheme that synchronizes and fixes an object point during rotation, without the use of an optomechanical object derotator. © 2002 Published by Elsevier Science Ltd.

Keywords: Electronic speckle pattern interferometry; Twin pulsed laser; Vibration and rotation fringes

1. Introduction

Speckle decorrelation on a moving object is a major problem in a dynamic electronic speckle pattern interferometry (ESPI) system. In particular for a rotating object, speckle decorrelation is present if the object angular displacement is larger than the average speckle diameter on the CCD sensor. Some solutions to this

*Corresponding author. Fax: ++52-4-717-50-00.
E-mail address: fmendoza@foton.cio.mx (F.M. Santoyo).

0143-8166/02/$ - see front matter © 2002 Published by Elsevier Science Ltd.
PII: S0143-8166(02)00007-6

problem have been proposed [1–4], in particular the use of two laser pulses to freeze the object movement between two different object positions. Fringes from a rotating object relate mainly to (a) deformations solely due to its rotation, for instance stresses due to the centrifugal force and out-of-plane vibrations, among others, and (b) the object angular displacement. Several research works report on methods to eliminate the rotation fringes by using an optomechanical derotator and on-axis illumination setups [5,6]. The use of the former devices requires a great deal of manipulation and hence is time consuming. Here, an alternative method to analyze object displacements in dynamic conditions, particularly while rotating, is presented.

The method is based on a high precision scheme that synchronizes [7] and fixes an object point during rotation. The interferometer is set to be sensitive to out-of-plane rigid body displacements by employing two laser pulses that illuminate the object along the rotation axis. For the analysis, the inherent rotation fringes may be seen as carrier fringes. A small object angular displacement between the firing of two laser pulses converts into a slope of the out-of-plane displacement, which is added to the carrier fringes, i.e., fringes due to out-of-plane displacement are modulated by the carrier fringes. As is customary, in addition to pulsed ESPI, the speckled interference patterns obtained from each of the pulses are added in a single frame of the CCD camera. Addition fringes are noisy and thus difficult to see on the monitor. However, in order to recover addition fringes at video rate, an analogue electronic filter [8,9] is employed. The method shows that any object unbalance may be detected by simply observing the changes in angular direction and frequency of the carrier fringes. With this method, there is no need to perform a phase calculation to obtain a displacement measurement, since the latter is achieved by time tracking the object vibration with respect to a rotating axis.

2. Principle of the method

The mathematical model for addition fringe formation in pulsed ESPI will be briefly described, since it may be found elsewhere, viz., [2]. Assume an unknown object displacement while it rotates, and that two laser pulses are fired within a CCD frame. All variables have (x, y) dependence, where coordinate axes (x, y) are fixed at the center of the CCD camera faceplate. The intensity on the CCD faceplate for pulse 1 is

$$I_1 = I_o + I_r + 2\sqrt{I_o I_r}\cos(\phi) \tag{1}$$

and for pulse 2,

$$I_2 = I_o + I_r + 2\sqrt{I_o I_r}\cos(\phi + \Delta\psi + \rho), \tag{2}$$

where as usual, I_o and I_r denote the object and reference beam intensity, respectively. ϕ is the random speckle phase, $\Delta\psi$ is the phase term due to object deformation alone, $\Delta\psi = 4\pi\delta z(t)/\lambda$, and ρ is the phase term associated to object rotation. Notice that Eq. (1) assumes that the object is rotating, but its motion is frozen during the 15 ns laser pulse width such that the equation does not contain $\Delta\psi + \rho$. Eq. (2) does

contain these phase terms since the second pulse is fired some microseconds after the first pulse, i.e., the object rotated and displaced. The addition of both pulsed speckle interferograms is done within a CCD frame, giving

$$I_t = 2(I_o + I_r) + 4\sqrt{I_o I_r}\cos\left(\phi + \frac{\Delta\psi}{2} + \frac{\rho}{2}\right)\cos\left(\frac{\Delta\psi}{2} + \frac{\rho}{2}\right). \quad (3)$$

In practice, the object beam lies in the $x'z'$ plane, coordinate axes set on the object, in such a way that the phase variable ρ can be uniquely expressed in terms of the y' object coordinate as

$$\rho = \frac{2\pi}{\lambda}(y' \sin\alpha)\theta. \quad (4)$$

The angle θ is chosen such that ρ represents, through Eq. (4), the object rotation contribution to the interferometer out-of-plane sensitivity vector, i.e., θ is small. Besides, θ allows for the formation of vertical carrier fringes. The angle α is the object rotation angle between pulses 1 and 2, with elapsed time t. This angular displacement renders rotation fringes under the following condition:

$$t < \frac{\lambda F}{2\pi\,\omega\,R}, \quad (5)$$

where λ is the wavelength of the laser light used, F is the f-number of the ESPI system imaging lens, ω is the object rotation frequency, and R its radii. The idea in using the fringes obtained in rotation as carrier fringes, to be later distinguished from out-of-plane displacement fringes, allows the displacement data $\delta z(t)$ to be analyzed as a change in fringe angular direction and frequency. To avoid the speckle decorrelation effects imposed by Eq. (5), the interferogram in Eq. (3) should be taken within that time limit. Experimentally and in present day applications, only shorter time separations, than those expressed in Eq. (5), are of interest.

The addition interferogram, Eq. (3), is electronically filtered so that it may be represented by a cosinusoidal fringe pattern, I_f. In fact the filter is designed to eliminate the first cosine term, a high frequency term [10], in the equation. Thus the argument of the cosine function that remains is the sum of $\Delta\psi$ plus ρ. The time lapse between the two pulses is of the order of 1 μs, allowing us to introduce in $\Delta\psi$ the slope of the object displacement as a function $\delta z(t)/\delta t$. This slope is evaluated at the same object angular position, e.g., each time the object completes one revolution. The final filtered speckle interferogram I_f depends on the slope of the temporal object displacement:

$$I_f = K\cos(b\delta z(t)/\delta t + \rho/2), \quad (6)$$

where K is a filter constant that depends mainly on the filter gain, and $b = 2\pi\delta\, t/\lambda$. It can be seen from Eq. (6) that the out-of-plane object displacement and rotation influence the frequency and angular direction of the resulting fringes. The out-of-plane object displacement is directly related to the object out-of-plane tilt over the $x'z'$ and $y'z'$ planes.

As mentioned, it is necessary to acquire the twin pulsed addition speckle interferograms at the same object angular position. The synchronization method

used in order to study the same object position is depicted in Fig. 1, whose top shows the CCD camera even and odd fields that would contain interferometric data. There are three conditions that the synchronization has to meet in order to have laser pulses falling inside CCD camera fields. (A) The CCD camera used has a NTSC system at 30 frames per second, so the laser has to deliver pulses at 60 Hz, even when the object rotating position is not the expected, a point widely explained in Ref. [7]. (B) In order to have interferometric data in the CCD camera fields, the object rotation frequency ω has to be equal to that of the external signal synthesizer. It should be noticed that some of the CCD camera fields have no information. (C) The twin laser pulses should be fired within to the initial and final CCD camera field, i.e., the laser should be synchronized with the camera. Finally, once the above conditions have been met, a pulse delay unit is used to visually freeze the object rotating motion, as seen on the TV monitor of the ESPI system, so that every image is captured at the same object position. A diagram block of the above procedure is shown at the bottom of Fig. 1. The synchronization operation accuracy was visually checked, a feature that is easily seen on the TV monitor by freezing the object rotation on the screen.

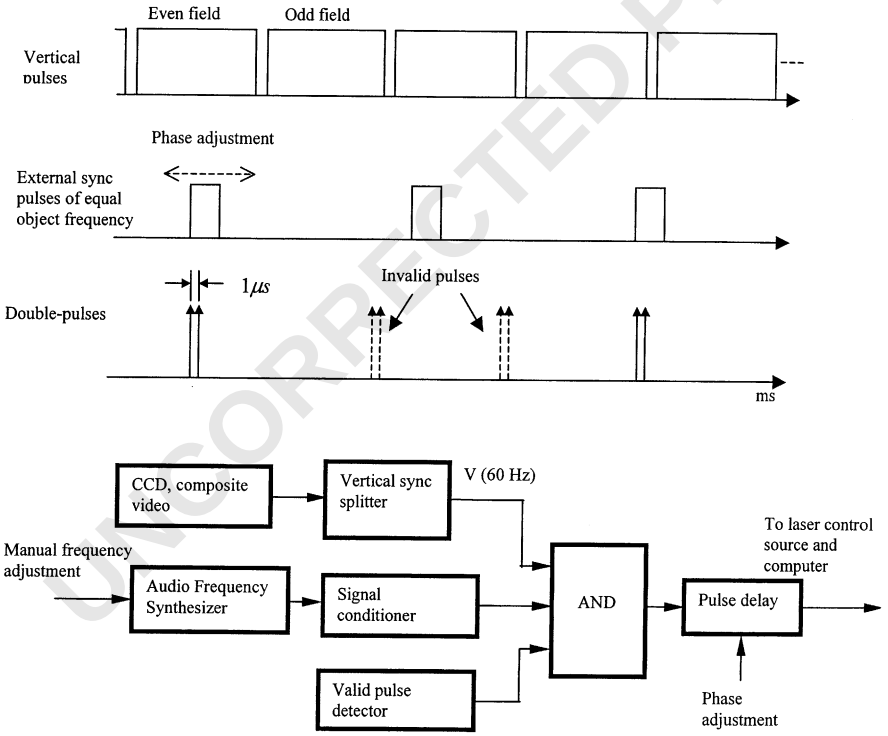

Fig. 1. Schematic diagram for the syncronization method.

3. Experiments and results

A typical out-of-plane ESPI arrangement is show in Fig. 2. Light from a Nd:YAG twin pulsed laser is divided in two at the beam splitter BS, to be used as the reference and object beams. The illuminated rotating object is imaged onto a CCD camera by a zoom lens. Previously, an object beam calibration is needed to reduce the rotation fringes to only three vertical fringes. The object under study is a rotating fan, whose blades rotate at $\omega = 1200$ rpm. The blades are considered to be plane and perpendicular to the line of observation. The laser was operated at approximately 20 mJ per pulse, with $\lambda = 532$ nm, 15 ns laser pulse width, and a pulse rate of 60 Hz. The CCD camera used had a faceplate with 640×480 pixels. A frame grabber inside a Pentium III PC is instructed to capture the speckle interferograms corresponding to Eqs. (1) and (2), for out-line processing.

A computer fringe simulation is shown in Fig. 3, where Eq. (6) was used to perform the calculations. Fig. 3a shows fringes due to rotation only, $\rho/2$. Fig. 3b has an object out-of-plane tilt along the $x'z'$ plane. Notice that this tilt increases the fringe frequency only. In Fig. 3c, an out-of-plane combination on both $x'z'$ and $y'z'$ planes has been added, a feature that shows a change in the angular direction of the fringes. For Fig. 3d, an out-of-plane object tilt was introduced along the $y'z'$ plane,

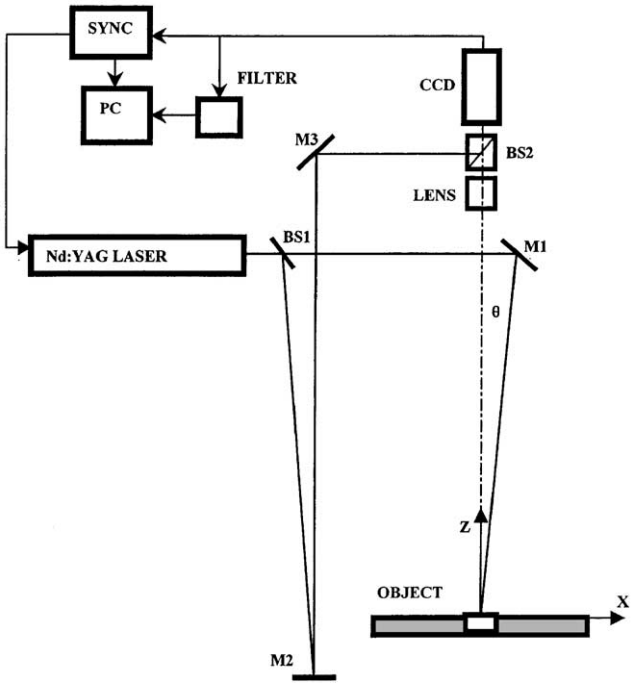

Fig. 2. Out-of-plane twin pulsed ESPI set-up as used for the vibrating analysis of rotating objects. BS1–2 are beam splitters, and M1–3 mirrors.

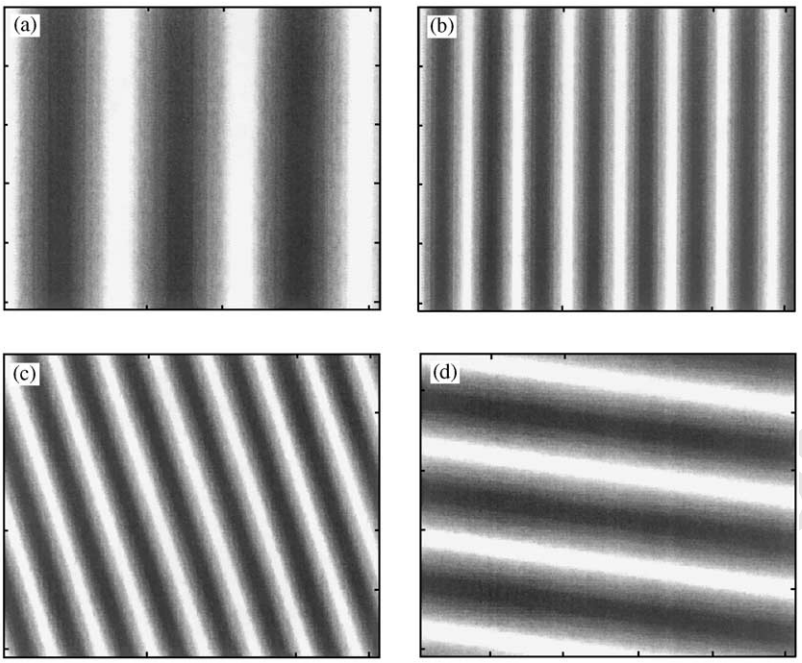

Fig. 3. Computer simulated fringes with an out-of-plane tilt introduced in b–d.

together with a subtraction of the term for object rotation. These figures were calculated with the purpose of emulating the experimental results to be shown next. For the case of a harmonic vibration of the rotating object, fringe patterns will be cyclic, meaning that if Fig. 3b represents a starting point, this pattern will repeat after some time. The time chosen for the computed images was 10 s.

The synchronization scheme explained before, allows the image acquisition with a predefined time pulse separation $t = 900$ ns, such that each object blade is seen exactly at the same position when each of the two pulses are fired. The synchronization yields a typical addition interferogram shown in Fig. 4a. The successive images are taken from exactly the same, apparently static, object position. The electronic filtering was made with a RC high pass filter, matched to a diode envelope detector to adapt TV positive voltages. Fig. 4b shows the filter action when detecting carrier fringes with the object rotating at 1200 rpm. Even with the characteristic additive noise, three vertical carrier fringes due to rotation can be observed on the TV monitor. In Fig. 4c, an object tilt along the y' axis, as described by Eq. (6), produces an increment in the vertical fringe frequency. Figs. 4d and e show a tilt combination on both x' and y' axes, affecting the angular direction and frequency of the fringes. In Fig. 4f, there is an object tilt contribution in x', however the y' tilt is in the opposite sense to the one for the carrier fringes, showing a near-horizontal fringe pattern. The images in Fig. 4 were taken in a lapse time of 10 s.

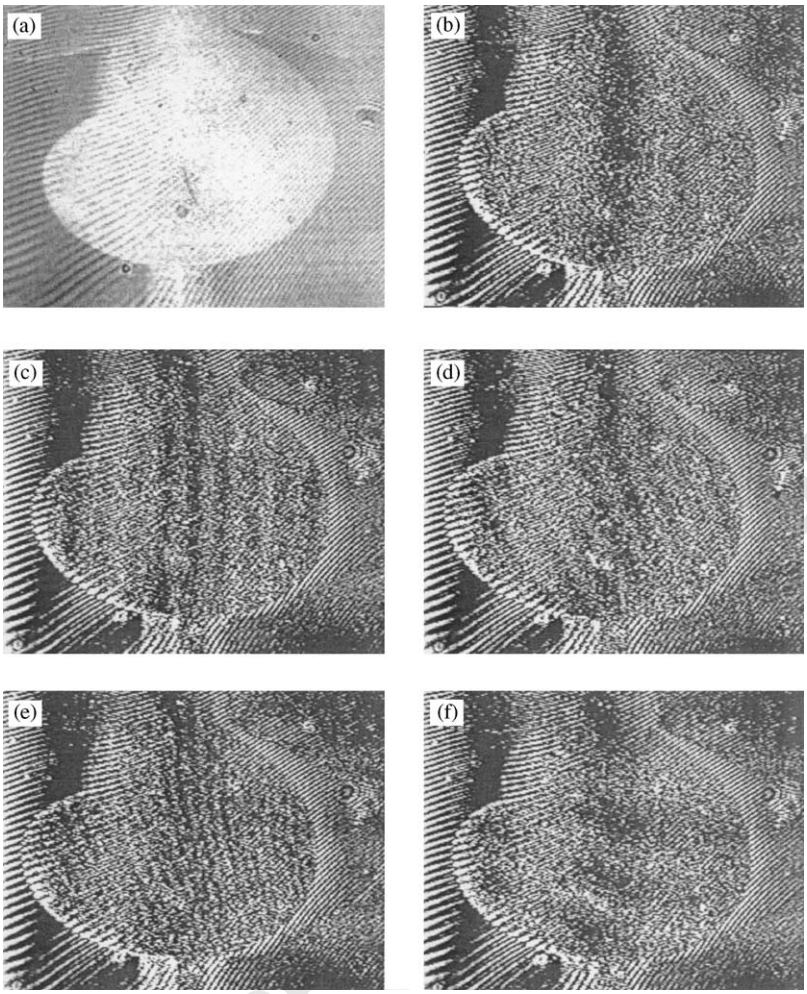

Fig. 4. A frozen blade of the rotating fan is shown. Out-of-plane tilt fringes may be observed in c–f. Compare these images to the ones in Fig. 3.

4. Conclusions

The addition ESPI method presented shows that it is possible to qualitatively study out-of-plane vibrations at video rate for rotating objects. The method is capable of separating vibration fringes from the inherent rotation fringes when a controlled synchronization and illumination arrangement are used. The advantage of directly watching on a TV monitor the addition interferogram, electronically filtered, allows reducing the time lapse between two images to obtain slopes of instant object displacement. Further considerations will have to take into account the blade shape, and simultaneously illuminated object points in order to obtain 3D

displacement vectors. Absolute measurement of displacements requires the inclusion of a z position controller. The method is suited to study out-of-plane vibrations in noisy environments. Finally, future research along the lines of this paper will be carried out shortly in order to quantify the data obtained with the aforementioned method, and to evaluate the system uncertainty with respect to the object angular position accuracy which was beyond the scope of the research results presented here.

Acknowledgements

This work was financially supported by Consejo Nacional de Ciencia y Tecnología (CONACYT), México, through grant 32709-A. We would like to thank Dr. A. J. Moore, Herriott Watt University, for his useful comments in one of the experiments.

References

[1] Cookson TJ, Butters JN, Pollard HC. Opt Laser Technol 1978;10:119.
[2] Shellabear MC, Santoya FM, Tyrer JR. Proceedings of the SEM Conference on Hologram Interferometry and Speckle Metrology. In: Pryputniewicz RJ. Editor. Processing of addition and subtraction fringes from pulsed ESPI for the study of vibrations, 1990, p. 238–44.
[3] Pedrini G, Pfister B, Tiziani H. Double pulse-electronic speckle interferometry. J Mod Opt 1993;40(1):89–96.
[4] Preater RWT, Swain R. Fourier transform fringe analysis of electronic speckle pattern interferometry fringes from high-speed rotating components. Opt Eng 1994;33(4):1271–9.
[5] Beeck MA. Holographic vibration analysis of rotating objects using different types of interferometers, SPIE 210, 2nd European Congress on Optics Applied in Metrology 1979,p. 128–34.
[6] Stetson KA. The use of an image derotator system in hologram interferometry and speckle photography of rotating objects. Exp Mech 1978;18:67–73.
[7] Moore AJ, Perez-Lopez C. Low-frequency harmonic vibration analysis with double pulse addition ESPI. Opt Eng 1996;35(9):2641–50.
[8] Moore AJ, Pérez-López C. Fringe visibility enhancement and phase calculation in double-pulsed addition ESPI. J Mod Opt 1996;43(9):1829–44.
[9] Ochoa NA, Santoyo FM, Moore AJ, Pérez-López C. Contrast enhancement of electronic speckle pattern interferometry addition fringes. Appl Opt 1997;36(13):2783–7.
[10] Ochoa NA, Santoyo FM, Pérez-López C, Barrientos B. Multiplicative electronic speckle pattern interferometry fringes. Appl Opt 2000;39(28):5138–41.